Millimeter-wave Ink-jet Printed RF Energy Harvester for Next Generation Flexible Electronics

Jo Bito*, Valentina Palazzi†, Jimmy Hester*, Ryan Bahr*, Federico Alimenti†, Paolo Mezzanotte†, Luca Roselli†, Manos M. Tentzeris*

*School of Electrical and Computer Engineering, Georgia Institute of Technology, Atlanta, GA 30308 USA

†Department of Engineering, University of Perugia, Perugia, Italy

***Abstract*—In this effort, the authors present the first demonstration of a flexible, inkjet-printed mm-wave rectenna. The design considerations and processes of the individual antenna array and rectifier are described, demonstrating a realized gain of 5 dBi, and a single-lumped-component via-less rectifier with up to a 2.5V dc voltage for an input power of 18 dBm, at the operation frequency of 24 GHz. The printed system is finally demonstrated in a wireless operation test, in a bent condition, thereby setting the foundation for the emergence of mm-wave-powered smart skins and wearables for the Internet of Things (IoT).**

***Index Terms*—energy harvesting, wireless power transfer, IoT, millimeter-waves, rectenna, rectifying circuit, flexible electronics, printing electronics.**

I. Introduction

The rapid growth of the seemingly independent fields of mm-wave technologies and IoT have produced large sets of high performance components and tools, as well as new avenues for the introduction of novel systems concepts and applications. The last decade has also witnessed the multidisciplinary-driven progress of flexible electronics, whose appeal for the low cost environmentally-friendly fabrication of wearable systems and ubiquitous smart skins has already motivated its use for numerous IoT systems [1] [2]. Yet, printed flexible mm-wave systems still remain largely absent, despite their potential for spatially-multiplexed long-range sensing, or highly-directed wireless power delivery, in addition to their relatively limited health hazard (apart from adverse low-depth heating effects at extremely high power densities) [3]. So far, tremendous effort has been put into the design of RF energy harvesters operating below a few GHz range, such as VHF, UHF and UMTS for broadcasting and cellular communication [4], [5]. In this effort, the authors propose the first reported prototype of a printed mm-wave rectenna on a flexible substrate, thereby opening the door to mm-wave-powered or triggered IoT wearables or smart skin motes. A system overview is given in the Sec. II, before the design of the two parts of the system, the antenna array (in Sec. III) and the rectifier (in Sec. IV), is described. Finally, the performance of the individual components, as well as that of the wireless operation of the entire printed system, are reported in Sec. V, before a conclusion is drawn in Sec. VI.

II. System Overview

The block diagram of the proposed mm-wave energy harvester is depicted in Fig. 1. The electromagnetic signal at 24 GHz is captured by an antenna and delivered to a rectifier. The latter consists of an input matching network, aimed at guaranteeing the impedance matching to achieve the maximum power transfer to the load, a rectifying element, which is here implemented with a diode, a harmonic termination section, thanks to which the RF components are isolated from the dc component, and the dc load. Bearing in mind the challenges of millimeter-wave operation, signal-to-ground vias, which entail the presence of highly-impacting parasitics, have been done without by introducing a via-less dc return path.

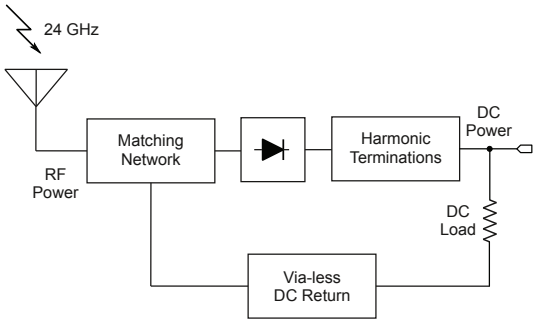

Fig. 1. Block diagram of the proposed rectenna.

The whole rectenna has been fabricated by using a flexible liquid crystal polymer (LCP) substrate (substrate thickness=0.18 mm, $\epsilon_r = 3$ and $tan\delta = 0.002$), while the microstrip traces have been fabricated by the ink-jet printing of a silver nano-particle ink. To this purpose, a Dimatix DMP-2831 ink-jet printer was utilized.

III. Antenna Design

As an antenna element, a planar 2×2 patch array has been chosen. Fig. 2 illustrates the antenna layout with the main antenna dimensions. The four patches are connected through a corporate feed network with three T-junctions and lie on the same layer as the $50\,\Omega$ input feeding line.

IV. Rectifier Design

A. Diode Characterization

The rectifying element of the present rectenna consists of a gallium arsenide beam lead Schottky barrier diode from Macom (MA4E2038 model). This diode has been chosen for its low series resistance and high cut-off frequency, which enable diode usage up to mm-wave applications. Nevertheless, the spice parameters provided by the datasheet do not include any of the parasitics associated with the diode package. Moreover, this characterization was not considered accurate enough at high frequency in previous works (see [6]). As a consequence, a performance study of the diode model was

978-1-5090-4585-3/17/$31.00 ©2017 IEEE

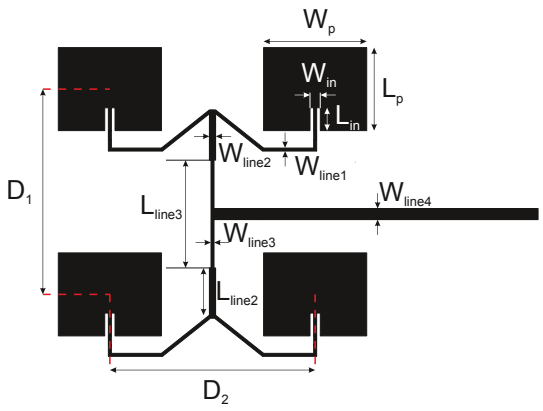

Fig. 2. Antenna layout. The main dimensions are: $W_p = 3.46\,\text{mm}$, $L_p = 4.3\,\text{mm}$, $W_{in} = 0.43\,\text{mm}$, $L_{in} = 0.95\,\text{mm}$, $W_{line1} = 0.125\,\text{mm}$, $W_{line2} = 0.259\,\text{mm}$, $W_{line3} = 0.125\,\text{mm}$, $W_{line4} = 0.46\,\text{mm}$, $L_{line2} = 2.03\,\text{mm}$, $L_{line3} = 4.5\,\text{mm}$, $D_1 = 8.6\,\text{mm}$, $D_2 = 8.6\,\text{mm}$.

conducted, in order to achieve a more accurate design of the rectifier.

Firstly, the diode dc characteristic was verified by testing three different diodes (see Fig. 3). A fine tuning of diode parameters, such as saturation current (Is), series resistance (Rs) and ideality factor (N), was carried out to achieve a better agreement between model and measurements.The package parasitics, represented by a series inductance and a parallel capacitance (as shown in Fig. 4), were estimated by using the values reported in a different datasheet for a diode with the same package. A comparison between the datasheet-based and the custom model is reported in Table I. The junction capacitance and all the other spice parameters have not been modified.

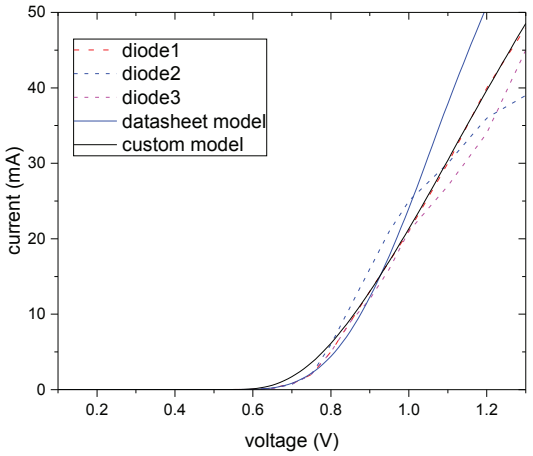

Fig. 3. Diode dc characterization.

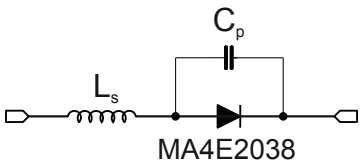

Fig. 4. Diode model with a parasitic inductor and capacitor.

TABLE I: Diode model: comparison between datasheet and optimized version.

diode parameters	datasheet	optimized model
Is	95 fA	10 fA
Rs	5.1 Ω	9 Ω
N	1.16	1
Ls	/	0.3 nH
Cp	/	0.011 pF

B. Rectifier Design

The final rectifier layout is reported in Fig. 5. Its input matching network consists of a distributed L-network, represented by a series line and a shunt stub. The stub is terminated by a virtual short-circuit for the fundamental and the second harmonic components, which is achieved by using quarter-wave open-circuited radial stubs. The same technique is used in the harmonic termination section. The dc return is obtained from the ring shape of the rectifier lines. A load equal to 739 Ω was identified, via optimization, for the maximization of the output dc power.

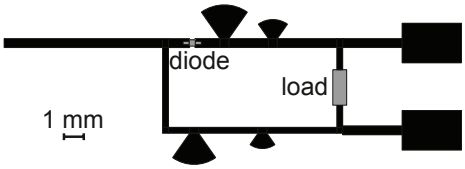

Fig. 5. Rectifier layout.

V. Measurement Results

A. Antenna Measurements

The measured input reflection coefficient of the antenna, reported in Fig. 6, features a slightly up-shift of the center band with respect to the simulated one. This effect, together with the matching worsening, is mainly due to fabrication process imperfections.

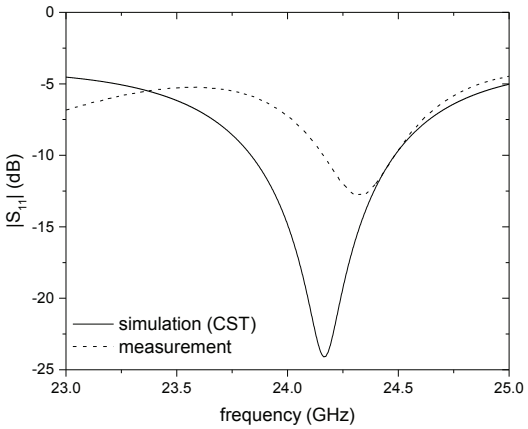

Fig. 6. Antenna input reflection coefficient: comparison between simulation and measurement.

Fig. 7 depicts the measured radiation pattern of the patch antenna prototype in $\phi = 0°$ and $\phi = 90°$ direction. The antenna prototype exhibited a realized gain of 5 dBi, wirelessly

measured using a 26.5 to 40 GHz conical horn antenna, YLB-28-20 from A-INFO, as reference.

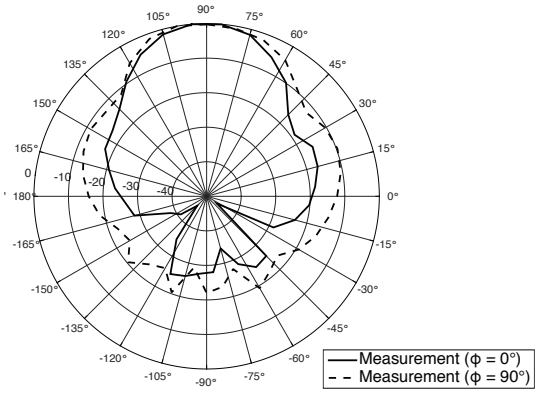

Fig. 7. Measured radiation pattern of the patch antenna prototype at 24 GHz.

B. Rectifier measurements

The output voltage of the rectifier prototype was measured with the aforementioned optimal 739 Ω dc load resistance. The comparison of measured and simulated output dc voltages with different diode models (custom and datasheet) with respect to the RF input power is depicted in Fig. 8. According to the figure, the simulation results show better agreement with the custom diode model than with the diode model from the datasheet.

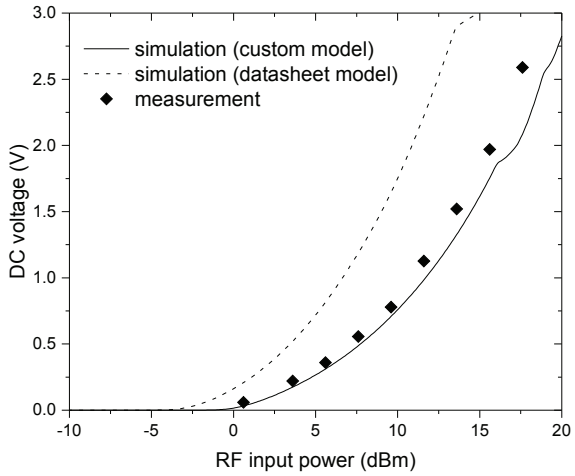

Fig. 8. Rectifier performance: output dc voltage versus RF input power.

C. Wireless Operation Test

As depicted in Fig. 9, a rectenna prototype was fabricated on a single LCP substrate for wireless operation tests combining the patch antenna and the rectifier characterized above.

As shown in Fig. 10 (a), the conical horn antenna, which was connected to a 26 dB gain amplifier, interrogated the rectenna prototype, creating an open output voltage of 0.286 V at 15 cm, using an expected output power of 29 dBm. Through a measurement depicted in Fig. 10 (b), an LED was successfully wirelessly turned on with the 24 GHz signal.

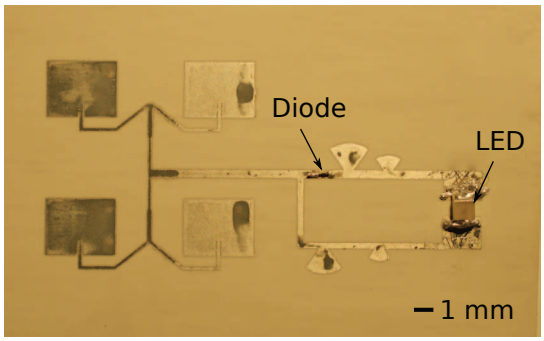

Fig. 9. Flexible 24 GHz rectenna prototype on LCP substrate.

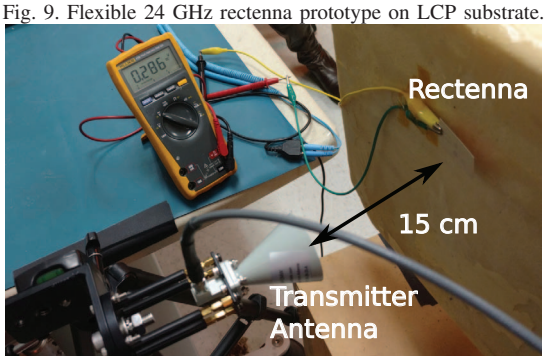

(a)

(b)

Fig. 10. (a) Wireless open output voltage measurement. (b) Wireless operation test with an LED under bent condition.

VI. Conclusion

In this paper, the diode characterization and the design process of a flexible inkjet-printed mm-wave rectenna were discussed. Both components were experimentally proven to provide adequate performance at the 24 GHz frequency of interest. The demonstrated ability to wirelessly deliver power through mm-wave channels opens the door for the emergence of energy-autonomous miniaturized wearables and smart skins for next generation fully-printed components of the IoT.

VII. Acknowledgment

The work of J. Bito, J. G. Hester, and M. M. Tentzeris was supported by National Science Foundation (NSF), Defense Threat Reduction Agency (DTRA), and Texas Instruments.

References

[1] J. G. Hester, S. Kim, J. Bito, T. Le, J. Kimionis, D. Revier, C. Saintsing, S. Wenjing, B. Tehrani, A. Traille, B. S. Cook, and M. M. Tentzeris, "Additively Manufactured Nanotechnology and Origami-Enabled Flexible Microwave Electronics," *Proc. IEEE*, vol. 103, no. 4, pp. 583–606, Apr. 2015.

[2] S. A. Nauroze, J. G. Hester, B. K. Tehrani, W. Su, J. Bito, R. Bahr, J. Kimionis, and M. M. Tentzeris, "Additively manufactured RF components and modules: Toward empowering the birth of cost-efficient dense and ubiquitous IoT implementations," *Proc. IEEE*, pp. 1–21, 2017.

[3] T. Wu, T. S. Rappaport, and C. M. Collins, "Safe for Generations to Come," *IEEE Microwave Mag.*, vol. 16, no. 2, pp. 65–84, Mar. 2015.

[4] S. Kim, R. Vyas, J. Bito, K. Niotaki, A. Collado, A. Georgiadis, and M. M. Tentzeris, "Ambient RF Energy-Harvesting Technologies for Self-Sustainable Standalone Wireless Sensor Platforms," *Proc. IEEE*, vol. 102, no. 11, pp. 1649–1666, Nov. 2014.

[5] V. Palazzi, C. Kalialakis, F. Alimenti, P. Mezzanotte, L. Roselli, A. Collado, and A. Georgiadis, "Performance analysis of a ultra-compact low-power rectenna in paper substrate for RF energy harvesting," in *Proc. IEEE Topical Conf. Wireless Sensors and Sensor Networks (WiSNet)*, Jan. 2017, pp. 65–68.

[6] S. Ladan, A. B. Guntupalli, and K. Wu, "A High-Efficiency 24 GHz Rectenna Development Towards Millimeter-Wave Energy Harvesting and Wireless Power Transmission," *IEEE Trans. Circuits Syst. I*, vol. 61, no. 12, pp. 3358–3366, Dec 2014.